Computer Simulation of Nanoparticle Aggregate Fracture

Takumi Hawa[1,2], Brian Henz[3], and Michael Zachariah[1,2]

[1]National Institute of Standards and Technology, Gaithersburg, MD, 20899
[2]University of Maryland, College Park, MD, 20742
[3]U.S. Army Research Laboratory, APG, MD, 21005

ABSTRACT

Nanoparticle aggregates have been found to possess unique mechanical properties. Aggregates of metal nanoparticles can be strained up to 100% before failure, and even typically brittle materials are observed to have a ductile failure mode. In this effort two materials; namely silver and silicon, were chosen to represent ductile and brittle materials, respectively. Aggregates with 2 to 6 particles were simulated using the molecular dynamics (MD) algorithm to determine the stress-strain behavior of the aggregate. Many interesting observations are made including the negligible affect of strain rate on ultimate tensile strength, and the direct relationship between Young's modulus and nanoparticle size.

INTRODUCTION

This effort is motivated by trying to gain an understanding of an AFM (Atomic Force Microscope) experiment [1]. In the experiment an AFM tip with a microsphere (radius ~ 12.5μm) of gold or silica attached was used to form a contact with a flat surface of the same material. Using a two nanoparticle aggregate of 5 nm diameter particles we have been able to simulate a system similar to this AFM experiment and measure the force required to separate the AFM tip from the surface after contact has occurred.

We have found the largest limitation of the computer simulations for aggregate systems to be the actual versus simulation strain rates. We are currently studying the effect of strain rate on the stress versus strain behavior of the nanoparticle aggregate. These results will provide a relationship for comparing simulation results at a high strain rate to experimental results at a much lower strain rate.

SIMULATION RESULTS

Using MD simulations we are able to compare results with an AFM experiment that collected force versus displacement data for an AFM tip bonded to a surface. This experiment is modeled as the straining of two sintered nanoparticles of like material. We then extended this model to investigate longer nanoparticle aggregates of up to 6 nanoparticles. These results along with some strain rate sensitivity investigations are presented in the following sections.

We also investigate the affect of another important aggregate parameter in this work, namely the primary particle diameter. The nanoparticle diameter affects many of the physical properties of the nanoparticle aggregate. Some of the parameters affected are the contact area, nanoparticle melting temperature [2], sintering time, and Young's modulus. Through MD

simulations we have been able to determine the relationship between nanoparticle diameter and contact area, a major determining factor in the maximum force for failure of a nanoparticle aggregate.

AFM Tip Experiment

In this experiment an AFM tip is brought into contact with a flat surface. A bond is formed between the tip and surface through interatomic forces. After the bond is formed the tip is pulled away from the surface and the force versus displacement is measured. A detailed description of these experiments for silica and gold can be found in Pradeep et al [1]. In order to model this experiment we simulate the tip-surface contact as contact between two nanoparticles. One limitation of the MD simulation is that whereas the AFM tip has a diameter of about 100 nm we are only capable of simulating nanoparticles with a diameter of about 10 nm in a reasonable amount of time. A comparison of the MD simulation and experimental results shows that qualitatively the MD results are able to predict the ductile behavior of the silica system, figure 1.
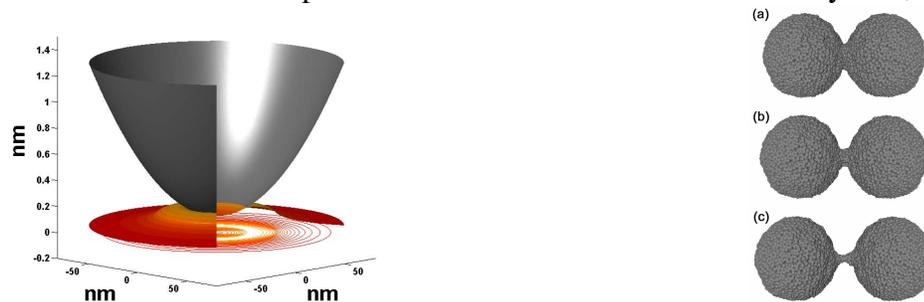

Figure 1. Illustration of AFM experiment showing AFM tip in contact with flat surface and the bonding that occurs [1]. Snapshot sequence (a), (b) and (c) from MD simulations demonstrates the material extension occurred during the separation for the silicon contact.

The conclusion that silica can break in a ductile manner is an interesting result because whereas gold is ductile at the macro-scale, silica in considered to be a brittle material. The reader is referred to Pradeep et al [1] for a more detailed discussion of this result. In attempting to simulate this experiment another limitation of the MD model was observed, that is the strain rate considered. A more detailed analysis of this issue is discussed in the following sections.

Strain Rate Affect

The greatest difficulty in performing these simulations is that MD simulations are limited in the amount of time that can be simulated. Using a time step of 1 fs (10^{-15}) requires 1 million time steps to simulate a single nanosecond of time. Therefore, the strain rates in this work are about $10^8 s^{-1}$. The affect of strain rate at these high levels is difficult to anticipate, but the most significant issue is that there is not time for atoms to diffuse into the neck region between the particles. This would most likely affect the length of the plastic strain region and not the computed Young's modulus from the elastic region which is unaffected by diffusion. On the other hand, at a slower strain rate more necking would be expected to occur as is observed in the AFM experiment.

We have investigated the affect of strain rate on Young's Modulus and ultimate tensile strength (UTS) for 5nm diameter Au and Si nanoparticles. The results of these simulations are tabulated in Figure 2.
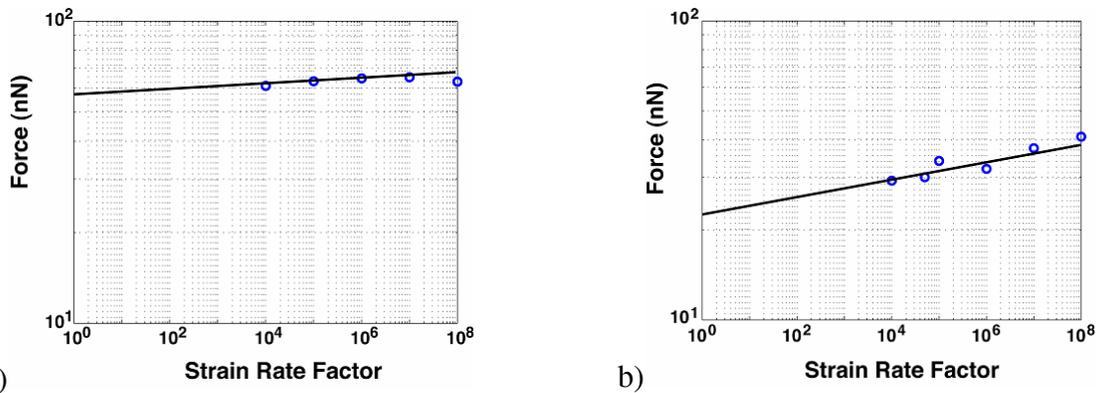
Figure 2. Maximum force before failure vs. strain rate for crystalline (a) and amorphous (b) silicon nanoparticle aggregates. The actual simulation results (open circles) and extrapolated results (solid line) are shown.

For the crystalline aggregate the maximum force prior to failure does not have a strong dependence on strain rate. This is observed by the relatively small, approximately 15%, drop in force for a 7 order of magnitude drop in strain rate. On the other hand, the amorphous aggregate shows a slightly stronger dependence on strain rate with a 40% drop in maximum force over the same range of strain rates.

Morphology

This effort considered the morphology, either crystalline or amorphous for nanoparticle aggregates formed by the sintering two nanoparticles. Figure 3 shows the computed force versus displacement curves for the crystalline and amorphous Si nanoparticles.
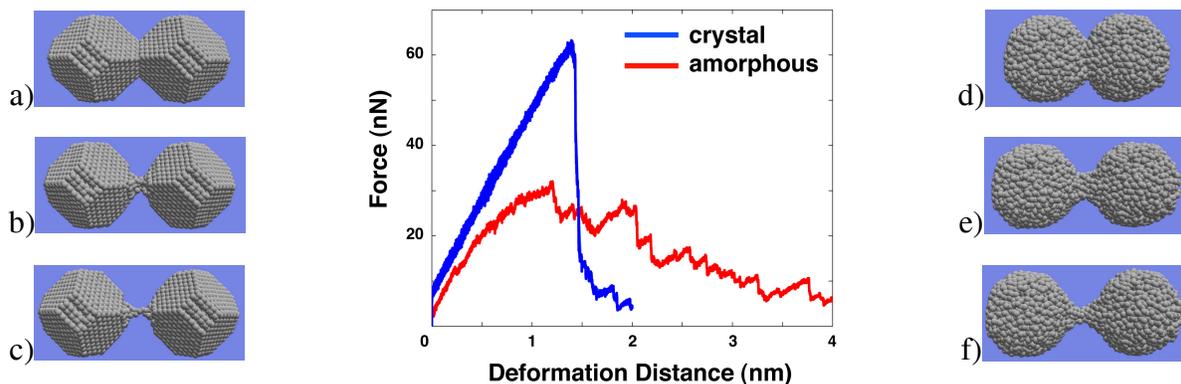

Figure 3. Force vs. displacement for MD simulation of crystalline (a-c) and amorphous (d-f) Si nanoparticles.

There are two interesting observations from the above simulation results. The first is that the Young's modulus appears to be unaffected by the nanoparticle morphology. This means that before necking occurs the slope of the force vs. displacement (stress vs. strain) curves have the same slope. The second observation is that the yield strength is much lower for the amorphous aggregate but more necking occurs prior to failure. This result is useful when deciding on a nanoparticle aggregate to be used in a system and suggests that morphology may be more

important than material since even silica exhibits ductile failure at these scales depending upon morphology.

__Aggregate Straining__

For the long chain aggregates silver is used in the place of gold. This was done solely for future experimental comparisons. The silver, as was the gold, nanoparticle aggregate is modeled using the embedded atom method (EAM) potential [3]. The EAM is used because it has been shown to accurately predict the mechanical properties of many FCC crystal lattice metals such as Au, Ni, and Ag. The EAM data used in this work comes from Baskes and Daw.

In this modeling effort there are four sizes of Ag nanoparticles considered, namely, 3, 5, 10, and 12 nm diameter nanoparticles. The first set of simulations involved placing two individual particles in close proximity so that through inter-atomic interactions the nanoparticles would sinter to form an aggregate. From these simulations we computed the contact area versus particle diameter for the 3, 5, and 10 nm diameter nanoparticles. The contact diameter turned out to be 1.7 nm or about 57% of the particle radius for the 3 nm diameter nanoparticle. The contact area was measured at 2.1 nm (40%) and 3.0 nm (30%) for the 5 and 10 nm diameter nanoparticles, respectively. These simulations were all carried out with a constant temperature of 300K. The equilibrated nanoparticles have faceted surfaces. As the nanoparticles increase in size these facets are less pronounced and the nanoparticle has a more spherical shape. This fact, in addition to the lowered melting point of the smaller nanoparticles, and the greater mobility of surface atoms contributes to the increased contact area at smaller nanoparticle sizes.

In the next set of simulations we formed longer aggregates of six nanoparticles each. Because of the large number of atoms in each 12 nm diameter nanoparticle, 53000 atoms, the six-particle aggregate of this size nanoparticle is not considered due to time constraints. Computation of the silver nanoparticle aggregate's Young's modulus was calculated as the slope of the stress versus strain simulation results. The stress tensor in these MD simulations is based on the virial theorem [4] computation. The stress component of interest is along the x-axis, σ_{xx}, because the other components are effectively zero in this analysis. The computed stress versus strain results and Young's modulus are shown in Figure 4.
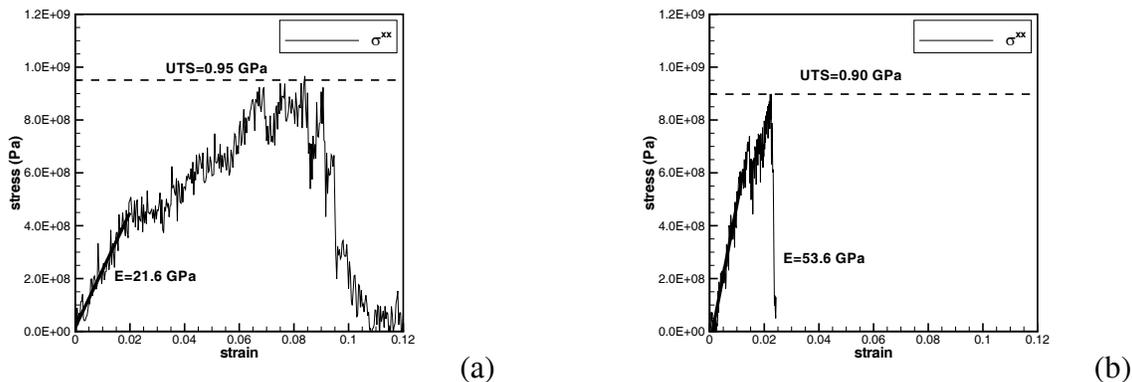

(a)   (b)

Figure 4. Stress versus strain plot for 6 particle aggregate of (a) 5 nm and (b) 10 nm diameter nanoparticles. Young's modulus (E) is plotted as slope in elastic region, and ultimate tensile strength (UTS) is denoted in plots.

In Figure 4 the Young's Modulus is computed to be approximately 21.6 GPa and 53.6 GPa for the 5nm and 10nm diameter nanoparticle aggregates, respectively. This value is about

25% and 65% of the bulk modulus of 83 GPa. A similar result has been observed for Cu nanoparticle aggregates [5] and Ni nanowires [6]. In addition, the ultimate tensile strength remains constant across the nanoparticle sizes investigated. The increase in the plastic region observed in Figure 4 between the 5nm and 10nm diameter nanoparticle simulations is possibly due to the difference in melting temperature of these particles. Since the predicted melting temperature of the 5nm diameter nanoparticle is lower than the 10nm diameter nanoparticle we would expect to see more diffusion of atoms occurring and resulting in more plastic strain.

During the mechanical testing simulation of the sintered nanoparticle aggregate the yield strength is reached and plastic deformation occurs. As the plastic strain increases, a neck begins to form and grow. The neck growth depends upon the nanoparticle size because in small nanoparticles the surface atoms are more mobile and diffuse into the neck region between nanoparticles. This diffusion maintains the neck thickness and prevents the rupture of the aggregate. Without the neck growth brittle fracture would occur with little or no measured plastic strain.

CONCLUSIONS

The results of the simulations of the fracture of nanoparticle aggregates presented here have some interesting observations. By comparing MD results with the AFM experiments of two sintered nanoparticles we have shown that even brittle materials may behave as ductile materials at the nanoscale. We have also shown that an inverse relationship between contact area and nanoparticle size exists. For the Young's modulus the opposite is true, as the nanoparticle size decreases so does the Young's modulus. The affect of strain rate on the Young's modulus was negligible as was morphology. The UTS is negligibly affected by strain rate for crystalline nanoparticles whereas amorphous nanoparticles are slightly more affected by the strain rate. The UTS is strongly dependent upon morphology with crystalline nanoparticles having a higher UTS. Although the strain before failure of crystalline nanoparticles is much lower than that of amorphous nanoparticles.

ACKNOWLEDGMENTS

REFERENCES

1. N. Pradeep, D.-I. Kim, J. Grobelny, T. Hawa, B. Henz, and M. R. Zachariah, *J. Applied Physics Letters*, (2007) (in press).
2. L. J. Lewis, P. Jensen, J.-L. Barrat, *Phys. Rev. B* **56**, 2248 (1997).
3. M. S. Daw, M. I. Baskes, *Phys. Rev. B* **29**, 6443 (1984).
4. J. H. Jeans, *The Dynamic Theory of Gases*, 4th ed. (Dover, New York, NY, 1960).
5. A. Dalis, S. K. Friedlander, *Nanotechnology* **16**, S626 (2005).
6. P.S. Branicio, J.P. Rino, *Phys. Rev. B* **62**, 16950 (2000).